INTERNATIONAL JOURNAL OF INTEGRATED ENGINEERING
ISSN: 2229-838X e-ISSN: 2600-7916

IJIE

Vol. 16 No. 5 (2024) 172-186
https://publisher.uthm.edu.my/ojs/index.php/ijie

Investigate The Applicability of Coating Titanium Substrate by Hydroxyapatite for Surgical Implants

Nabaa S. Radhi[1], Haydar H. Jamal Al-Deen[1], Rasha Safaa Hadi[1], Zainab S. Al-Khafaji[2,3]*

[1] *College of Materials Engineering, University of Babylon, Babylon, 51001, IRAQ*
[2] *Building and Construction Techniques Engineering Department, College of Engineering and Engineering Techniques, Al-Mustaqbal University, 51001, Babylon, IRAQ*
[3] *Department of Civil Engineering, Faculty of Engineering and Built Environment, Universiti Kebangsaan Malaysia, 43600 UKM Bangi, Selangor, MALAYSIA*

*Corresponding Author: p123005@siswa.ukm.edu.my
DOI: https://doi.org/10.30880/ijie.2024.16.05.014

Article Info

Received: 23 October 2023
Accepted: 31 May 2024
Available online: 1 August 2024

Keywords

Hydroxyapatite, biocompatibility, tissues in vivo, osseointegration, pulse laser deposition

Abstract

Pure titanium and titanium alloys are the materials that are utilized the most often for the production of dental implants, and hydroxyapatite is the bioactive substance that is most frequently coated on titanium implants. Ceramics are a family of biomaterials that include hydroxyapatite. This substance has structural and chemical similarities with biological apatite, the primary inorganic component of tooth and bone, and hydroxyapatite is also a ceramic. The substance is not only osteoconductive and non-toxic, but it also has bioactive properties. This research studied and manufactured a coating for surgical implants by employing hydroxyapatite (HA), a distinctive bone that grew at a medium for prosthetic human body parts. This coating was meant to boost bone development. Pulsed laser deposition (PLD) created titanium substrate HA coatings. This search employed HA compressed at 150 MPa with a particle size of 2.745 m as a coating target utilizing PLD methods with (8000, 6000, and 4000) pulses. SEM and AFM were used to describe the coating surface and determine calcium and phosphorus concentrations in the coating layer. In an in vivo study, four rabbits' femur bones were implanted with Ti-HA-8000, Ti-HA-6000, Ti-HA-4000, and Ti. Both groups showed new bone growth surrounding the implant at three weeks. Haversian lamellae indicate mature bone growth and complete osseointegration surrounding the Ti-HA-8000 implant after six weeks, which implies that HA is biocompatible and facilitates implant-bone osseointegration.

1. Introduction

The mechanical characteristics of titanium (Ti) and its alloys are more like those of bone than those of stainless steel or cobalt-chromium alloys; titanium (Ti) and its alloys are utilized as prosthetic joints and tooth roots in orthopaedic and dentistry applications. Until now, the mechanical differences between titanium and bone have had unfavourable consequences, such as stress shielding. For hard tissue implantation, several novel Ti alloys were created with an emphasis on managing the alloy element and its composition, phase, and other properties to lessen these impacts [1], [2]. It is a lengthy process to attach metal implantation to bone and achieve stability when it does not undergo surface modification to improve osteoconductivity. Several methods exist for enhancing the osteoconductivity of titanium and its alloys. These methods fall under one of the following two

categories: Metallic implantation is covered with bioactive substances that speed up bone production, and creating a rough microsurface on the metallic implants causes the implants to become anchored in the bone. Surface-modified implantation was employed in clinical settings, and these procedures have shown some success. However, there are still issues with the coating which require being addressed, as well as questions about how the surface characteristics affect osteoconductivity [3].

The development of the Pulsed Laser Deposition (PLD) process as an alternative to several coating techniques offers the additional benefit of maintaining the target phase's stoichiometry [4], [5]. The PLD process may produce the desired layer thickness, shape, and composition by adjusting the deposition settings. This method allows the deposition of several target materials with different physical, biological, and chemical properties on a substrate for functionally graded coatings [6], [7]. Bioceramic coatings are either bioactive (calcium phosphate/hydroxyapatite and bioglass) or bioinert (zirconia and alumina) [8], [9]. Bioinert ceramic coatings are more biocompatible and mechanically superior to other coatings. However, bioinert ceramics' high brittleness, elastic modulus, and limited tissue interaction limits their use in this industry. Calcium phosphate and bioglass are used more often to treat titanium implants because they improve implant-bone adhesion by interacting with tissues [10], [11]. However, titanium implants are the most common treatment.

Metallic implants have corrosion and strength issues [12]–[14]. Titanium composites, pure titanium, treated steel, and cobalt combinations are used as bone embeds owing to their excellent quality, sturdiness, and low in vivo corrosion rate [15]. Embed metals are biocompatible since they may be eaten in the body's hostile environment [16]. [17] found that bio-active HA (Ca10 (PO4)6(OH)2) coatings on metallic implants may reduce these problems. Hydroxyapatite (HAp) covers bioactive elements in metallic embeds with several benefits [18]. These benefits include better biointeraction with surrounding tissues and embedded surface erosion resilience [19], [20]. In vivo studies show HA-coated Ti improves implantation fixation in 3-6 months [21]. However, plasma-sprayed coatings have struggled to maintain phase purity and mechanical strength in vivo [22]. Due to its ability to quickly create a thin TiO2 coating of a few nanometers in thickness under typical air circumstances, titanium also demonstrates intrinsic biocompatibility [23]. According to reports, an interlayer of titania (TiO2) created using sol-gel techniques may increase the coating's adherence to the Ti substrate and the HA substrate [24], [25].

The surface chemistry of the bioceramic coating determines whether it will adhere to titanium implants and how well it will work with titanium implants. In many cases, the qualities of the bioceramics before the coating process are not the same as the attributes of the bioceramics after the coating procedures. The PLD approach is remarkable in that it offers many benefits, including the uniform deposition of particles in a short amount of time, the excellent adhesion of the coating to the substrate, and the maintenance of good stoichiometric and homogeneous phase transformation [26]. Kwiatkowska et al., [27] have previously reported on the PLD of bioactive glass; nevertheless, the powder they have utilized is of micron size and was created by the melt-derived technique. Compared to the generated approach, several prior research established that the sol-gel-produced bioactive glass is more favourable in boosting the biocompatibility of the material [18], [28]. So, this study aims to develop a method for synthesizing sol-gel-generated bioactive glass and applying it as a PLD coating on a titanium material. Similarly, past research on PLD of hydroxyapatite structures on titanium alloys [29], hydroxyapatite film [30], and polymer substrates [31] mainly focused on adhesivity characteristic and phase structure development of specimens after coating. According to Rajesh et al., [32], an interlayer of titania helped to create an adherent and stable HA coating over Ti6Al4V. By subjecting the interlayer to laser ablation at a substrate temp of 400 degrees centigrade, the interlayer was formed to a submicron level. HA was successively deposited to a thickness of about one micron. XRD, SEM, energy dispersive X-ray analysis, and inductively coupled plasma spectrometry determined that the deposited phase was phase pure HA.

Implants are commonly made of non-osteoconductive metals. Osteoconductivity permits bone to form on a material, indicating compatibility with surrounding bone tissue. Metal surface modification is done to improve hard tissue compatibility or bone development [33]. Biomimetic ceramics are famous in tissue and prosthesis engineering [34], [35]. Hydroxyapatite's ability to interact with living bone tissue and form strong bonds with bone is likely its most intriguing property. It is a bone-filling or metal implant covering in orthopaedics, dentistry, and maxillofacial surgery [36]. Other studies found that some hip prostheses and component components made of metals or metal alloys, notably titanium alloys coated with hydroxyapatite, stimulated implant bone development. Hydroxyapatite may be deposited on titanium alloys in several ways. Coating techniques include atmospheric plasma spraying, PVD, CVD, and other deposition processes [22], [37]. Like hot dip, chemical vapour deposition, and slurry methods, thermal spraying technology is an effective coating preparation process. Because it strengthens coating-alloy substrate bonding, this work examines the osteoconductivity and biocompatibility of titanium samples coated with hydroxyapatite layer utilizing pulsed laser deposition (PLD) on four rabbits' femur bones at three pulse densities (4,000, 6,000, and 8,000).

Int. Journal of Integrated Engineering Vol. 16 No. 5 (2024) p. 172-186

2. Implement Preparation Process

2.1 Pulsed Laser Deposition Technique

A verified physical vapour deposition method, Pulsed-Laser Deposition (PLD), produces high-quality multicomponent oxide thin films [16]. A 10–30 nanosecond laser pulse is emitted from a solid object. The laser swiftly elevated the surface temperature of a small quantity of the target beyond evaporation, and it was collected on a neighbouring substrate. The constant non-steadiness evaporation of multicomponent substances and the transfer of the target configuration to the deposited thin films create high-quality, accessible, and placeable thin films of materials that other PVD techniques cannot. Throughout this research, a titanium plate was split into three separate samples, each measuring (4.5x2.5x0.1) mm. The samples were then given a final washing in distilled water. After that, these specimens were decreased with acetone and ultrasonically cleaned with ethanol and acetone, respectively, utilizing an ultrasonic cleaning apparatus. The ultrasonic cleaning process lasted 10 min and used acetone as the medium. To prepare the HA target, 15 grams of nanopowder are combined with 3 mm of polyvinylalcohol (PVA), the binding ingredient. After that, the mixture was compressed using a device called a compacted apparatus and pushed at a pressure of 150 MPa to get the target that is illustrated in Fig. (1b). The mould was pre-lubricated to facilitate the process of releasing the smaller model and to lessen the amount of friction that occurred. Following that, the target was dried utilizing the dry box at a temperature of 150 degrees Celsius for four hours to dehumidify and release the PVA.

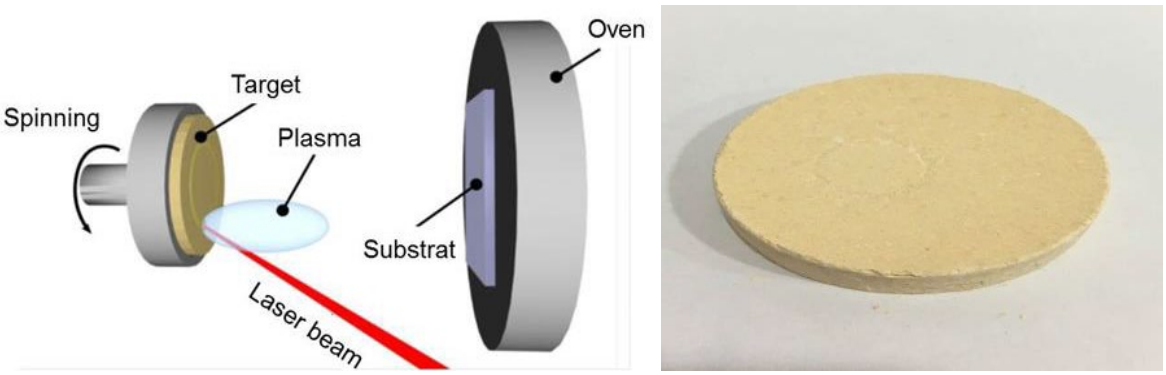

Fig. 1 *(a) Schematic of the PLD process; b) One of the targets after pressing proces [12]*

2.2 Deposition Procedure and Parameters

In order to meet the work goals outlined, the titanium specimens will first be coated with HA by the plan to obtain the Target pressure of 150 MPa and a substrate temperature of 300°C. HA deposition factor, Pulses equal (4000, 6000, and 8000), Power equals 1000 MJ, Frequency equals 6 Hz, Laser wavelength equals 1064 nm, Pulse time equals 10 sec, and Vacuum pressure equals 10 bar.

2.3 Tests

Throughout this investigation, the following evaluations have been carried out to assess the efficiency of the HA coating layer on the Ti substrate:

2.3.1 Thickness Test

The thickness of HA films on Ti substrates was measured using a thickness measuring tool at (Babylon/University of Babylon/College of the Material Engineering in Babylon).

2.3.2 Hardness Test

At the University of Babylon's College of Material Engineering, the Vickers Hardness (TH-717 Digital Micro Vickers Hardness Tester) has been utilized to evaluate the brittleness of HA films using a force of 300g and a holding time of 15 seconds.

2.3.3 Surface Roughness Test

A HA-coated Ti specimen's surface roughness was assessed utilizing the (TR-100 surface roughness tester) at the University of Babylon's Faculty of Materials Engineering. To detect the surface roughness, the instrument

moves over the specimen surface. The apparatus contains a sensor that captures the sample surface's roughness and reads the value immediately from the screen. The instrument's precision (± mμ0.01).

2.3.4 AFM Analyzer

In the (college of Material Engineering/University of Babylon) study, atomic force microscopy (AFM, interaction mode, spm AA3000 Angstrom Advanced Inc., USA) has been utilized to examine the morphology (roughness, morphological depth of films).

2.3.5 SEM Analyzer

In this piece of research, an electron scanning microscope, or SEM, is utilized to explore the materials' underlying microstructure in both their coated and uncoated forms. It has been utilized to describe the morphology and microstructure of the coated surface in terms of its uniformity, which was carried out at the (University of Technology / Department of Production and Metallurgy).

3. Experimental in Vivo Study

The specimens were formed into sheet forms throughout the fabrication process. Pilot trials are often used to test produced materials for their biocompatibility (the absence of harmful effects) and bioactivity (the capacity to integrate with the jawbone via osseointegration), both critical for implant applications. The term "in vivo research" refers to implanting live tissue. Because of this, the femur of a rabbit is often used as the host for the implantation. The in vivo study's surgical process, the work plan, substances, and several pieces of equipment used are discussed in this section of the report.

Due to the limited resources that are accessible in the surrounding area, both the hard (bone) tissue and the interface between the implantation and the hard tissue were checked at time intervals of no more than six weeks. This endeavour was assisted by two medical physicians (MDs) and one lab specialist (medical lab analysis), all of whom are acknowledged in the acknowledgements section. Investigations of the tissue around the implants were carried out at three and six weeks following the implantations, respectively [38].

Four implantations were used, and four animals, all of which were rabbits aged 12 to 15 months, were destroyed as a result. Fixation, decalcification, dehydration, infiltration, sectioning, and staining are the fundamental processes involved in preparing the tissue that will house the implant and the bone [39].

3.1 Sterilization of Implants and Surgical Instrument

Sterilization of the implantation and instruments is the first step that must be taken before the surgical process. Ti, Ti-coated with HAP of (4000, 6000, 8000), in addition to implantation, are all components of the sterilizing process. Polyethene sheeting that is airtight and an autoclave (HIRAYAMA HVE-50); following the procedure described in [14], one implantation was placed in a single airtight sheet, and the implantation was then autoclaved for thirty min at a pressure of twenty bar and a temperature of one hundred twenty degrees Celsius.

3.2 Surgical Process

Researchers used four rabbits of local provenance that ranged in weight from 1.6 to 2 kg each. The ages of the animals ranged from 12 to 15 months. These animals were housed in a conventional separate cage, given unrestricted access to running water, and fed regular pellets and veggies. They also had free access to the tap water. Before the surgical procedure, they were allowed to remain in the same setting for two weeks. The equipment underwent a 30-minute autoclaving process at 20 bars of pressure and 120 degrees Fahrenheit.

The amount of anaesthesia and antibiotic required was determined by weighing each rabbit using an instrument designed specifically for use with animals. A combination of ketamine and xylazine [40] was injected intramuscularly in order to induce anaesthesia. The operation was successful because of the sterile environment and the cautious approach used by the surgeons. Each rabbit's left hind leg was given a full-body shave with shaving spray from all angles. The surgical cloth was wrapped around the area that was being operated on. First, ethanol was utilized to clean the skin, and then the iodine was applied. Figs (2 (a, b, and c) show that a surgical towel has been utilized to wrap the leg.

Int. Journal of Integrated Engineering Vol. 16 No. 5 (2024) p. 172-186

Fig. 2 *Surgical clips and towels around the surgical site*

To expose the femur bone, an incision was made on the medial side of each leg, and its length was approximately 3 cm (3,b). Both the skin and the fascia were seen in the reflection. Careful reflection was done on the periosteum (vascular connective tissue), as seen in Fig. (2,c). Fig. (3) shows a reflection of the muscles and fascia. A round bar has been used with an interrupted pressure source to conduct the drilling operation. The hole's expansion was carried out in stages using a drill with a diameter of 3.2 mm; see Figs. (4) and (6).

Fig. 3 *Making a surgery for the rabbit to implant the implements in the rabbit's body*

The implantation has also been withdrawn from the plastic sheet and then inserted in the hole while applying a modest amount of pressure until it is fully introduced into the bone (see Fig. 3). Fig. 3 shows the

Int. Journal of Integrated Engineering Vol. 16 No. 5 (2024) p. 172-186

process of suturing (stitching) the fascia using absorbable Sutton sutures, which was then followed by suturing the skin. A local and systemic antibiotic was administered for five days following the operation in the postoperative therapy provided.

3.3 Histological Testing

Histological examination of the implant was carried out using an optical microscope. After sacrificing the animal by giving it an overdose of general anaesthesia after six weeks of healing intervals, bone sectioning was carried out on the specimens obtained from the sacrifice. While cutting the bone surrounding the implantation, a disc cutter with a slow rotational speed and aggressive cooling has been utilized. In order to get a bone-implant block for histological examination, the cutting was done farther than 1 cm away from the head of the implantation. Fig. (4) displays the bone-implant block used for the histological examination.

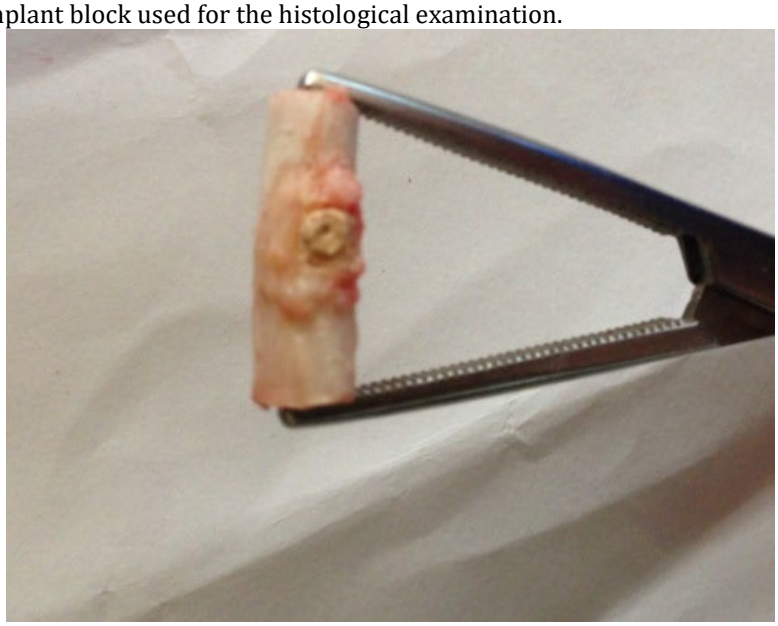

Fig. 4 *Bone-implant block for histological test*

The block of bone and implant was placed immediately into 10% freshly produced formalin and allowed to sit for one day. However, to prepare the material for histological sectioning, the following processes were carried out [33]: the samples were soaked in a solution containing 10% formic acid for approximately one week or a few more days to decalcify the bone. It altered the amount of acid allowed for examination of the bone. In addition, bone decalcification was examined by inserting a skinny needle into the interior part of the bone implant block. Once the process of decalcification was finished, the bone-implant block was cut in half using a sharp scalpel along the length of the implant inside the bone and through the implant, which was done in such a way that the bone was cut into almost two parts, one of which included the implant. After that, the implantation was removed from its bone bed in a very delicate manner. It was scrubbing the bone in a stream of deionized water to remove any remaining formic acid residue.

The tissue process is subsequent actions such as the sample was submerged in three various amounts of alcohol to accomplish the dehydration process: 70% (for one day), 90% (for 2 hrs.), and 100% (for 2 hrs.). After that, the specimens were soaked in xylene for two hours. Each sample was placed in its dish, filled with liquid paraffin and placed in an oven maintained at a temperature of 78 degrees Celsius. Throughout many hours, the sample was transferred into two or three successive paraffin dishes to completely supplant the xylene present in the tissue with paraffin.

Theffin was removed from the slide by heating it to 78 degrees Celsius in an oven for 30 to 45 min. The slide was then put inside the oven, where it remained for 15, 15, and 30 minutes in each of the three xylene jars. To eliminate any traces of alcohol, the slide was first submerged in alcohol in various amounts: 80% (for 3 min), 90% (for 2 min), and 100% (for 1 min). The slide was then rinsed in deionized water [41].

4. Results and Discussion

4.1 Thickness Results

The specimen with the designation (Ti-HA-4000) has a thickness of 2.2µm. In contrast, the sample with the designation (Ti-HA-6000) has a thickness of 3.2 µm, and the specimen with the designation (Ti-HA-8000) has a thickness of 4.15 µm. The deposition rate rose as the number of laser pulses increased, and the thickness grew due to an increase in the deposition layer due to an increase in the deposited quantity of HA, which increased proportionally with the rise in pulse number, as illustrated in Fig. 5.

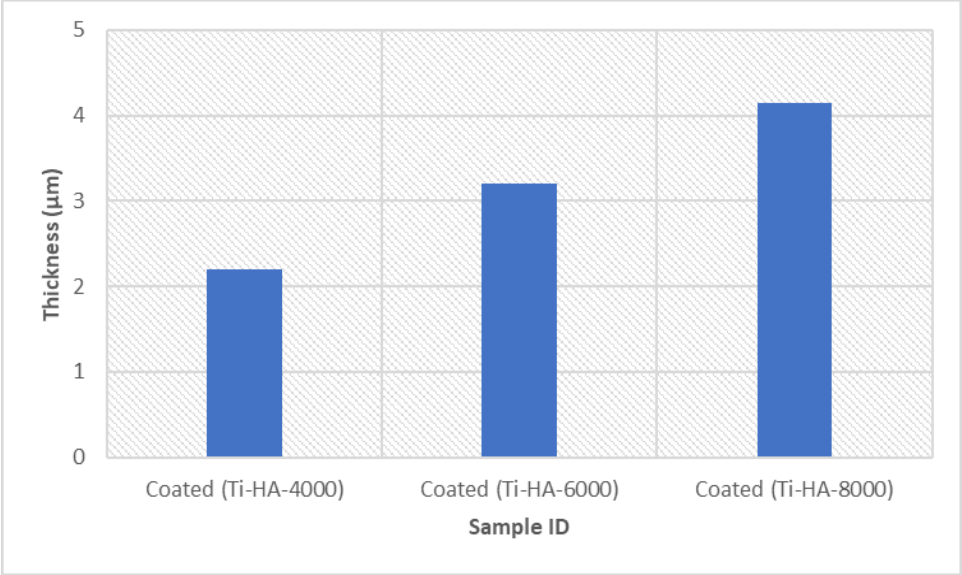

Fig. 5 *The HAP coating thickness layer for various pulses number of pulses*

4.2 Hardness Results

Fig. 6 illustrates how the number of laser pulses influences the hardness achieved by the HA coating. The number of pulses substantially impacts the final level of hardness achieved. After being treated with HA, uncoated samples have greater hardness than before. Additionally, increasing the pulses from 4000 to 6000 to 8000 improved the hardness from 247 HV to 252 HV to 277 HV. These results agree with Rajesh et al., [42], and this enhancement is attributable to the enhancement of depth morphology, distribution, and increase in HA thickness, all of which may be detected. The pulse lengthening will likely implant additional HA particles on the surface of the substrate.

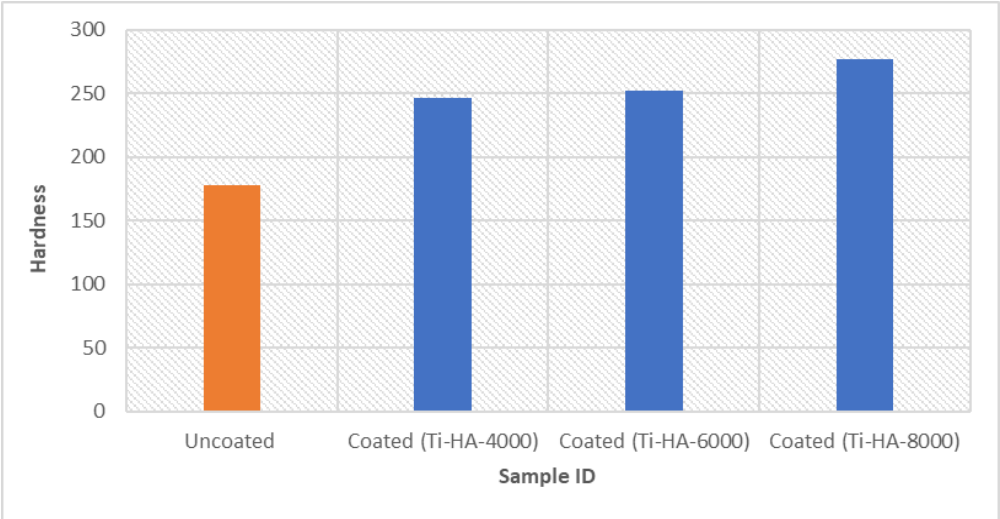

Fig. 6 *The influence of LPD on HA coating hardness (Hv)*

Int. Journal of Integrated Engineering Vol. 16 No. 5 (2024) p. 172-186

4.3 Roughness Test

The HA film roughness for the titanium sample with 4000 laser pulses was 0.482 µm, and it grew until it reached 0.510 µm for the titanium specimen with 6000 laser pulses. After that, the roughness increased until it reached its peak magnitude of 0.965 µm for the titanium specimen with 8000 laser pulses. Fig. 7 displays the impact that the total number of laser pulses has on the surface roughness of the HA coating.

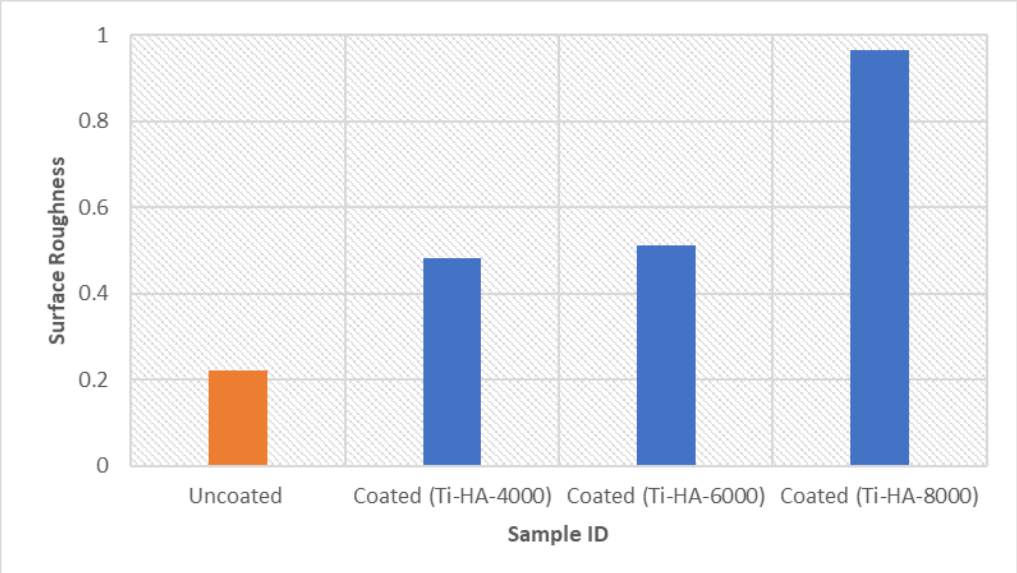

Fig. 7 *The influence of laser pulses on surface roughness of HA coating*

4.4 AFM Results

Fig 8 shows the findings obtained from the AFM examination of HA coatings that were applied using a variety of laser pulse intensities. It has been shown that raising the pulsed laser to a higher intensity (8000) affects the pace at which HA particles are deposited. It could be detected that the roughness increased with the pulses increasing to (8000); this agrees with the surface roughness measurement as shown in Fig. 7.

The 3D surface profile obtained in the atomic force microscope also showed a granular morphology (Figs 8). The peak-count histogram allowed for the estimation of the particle size range on the surface [40].

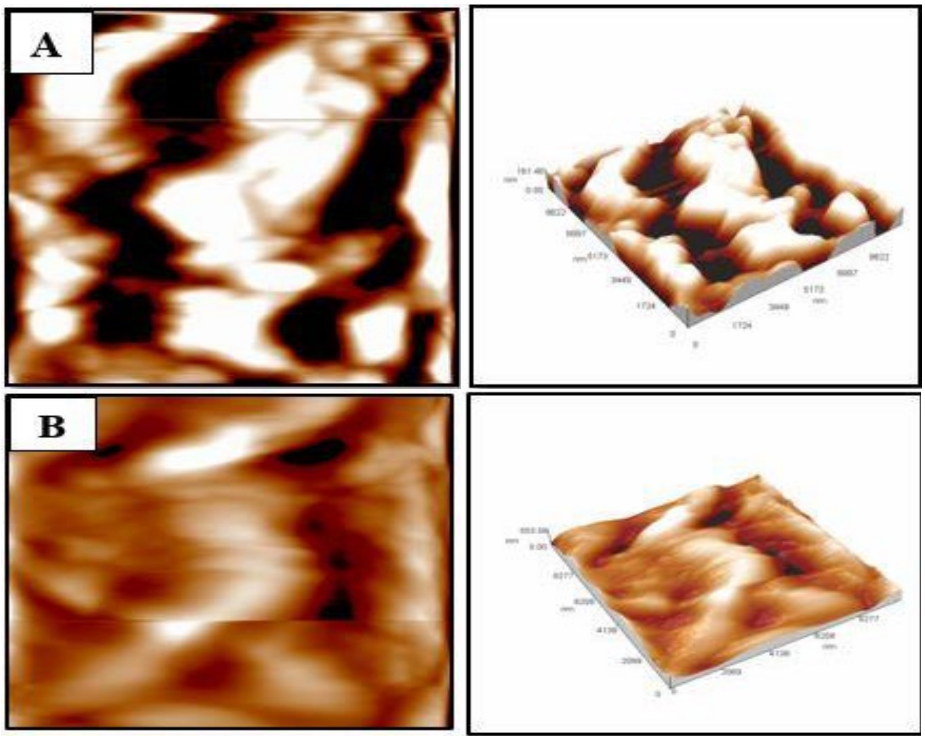

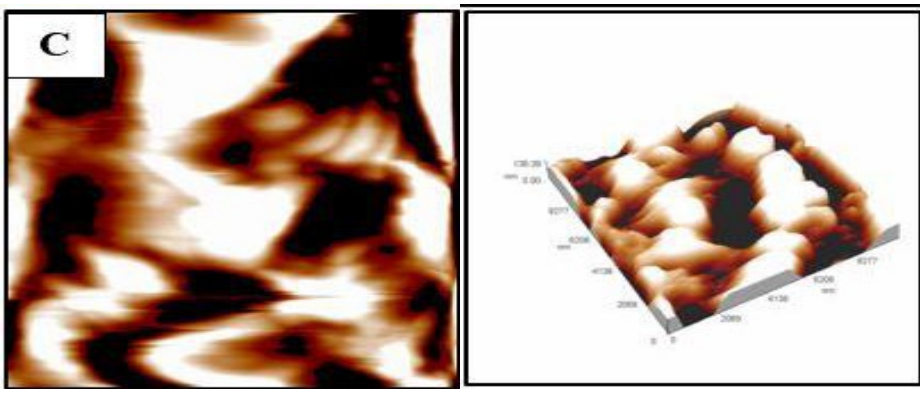

Fig. 8 *AFM pattern of samples at (a) (Ti-HA-4000); (b) (Ti-HA-6000); and (c) (Ti-HA-8000)*

4.5 SEM Results

After going through the PLD process, the substrate had white continuous coatings. The coating had the impression of being formed of globules of a few microns in size, had a white look, and displayed extraordinary homogeneity, according to SEM [40]. Surface profilometry performed on a coating applied over two hours yielded step thickness measurements of (2.2, 3.2, and 4.15) microns, depending on the number of pulses used. (4000, 6000 and 8000). The scanning electron micrographs of the 150MPa HA specimens that were deposited at various pulses and a substrate temp of 300 degrees Celsius are shown in Fig. 9. According to the Fig., it is evident that raising the pulse resulted in an enhancement of HA Films. On top of the base material, the HA particles are deposited to generate clusters that have the appearance of a dense and aggregated composition. In addition, increasing the number of pulses could be helpful in terms of enhancing the growing film as well as its density and microstructure.

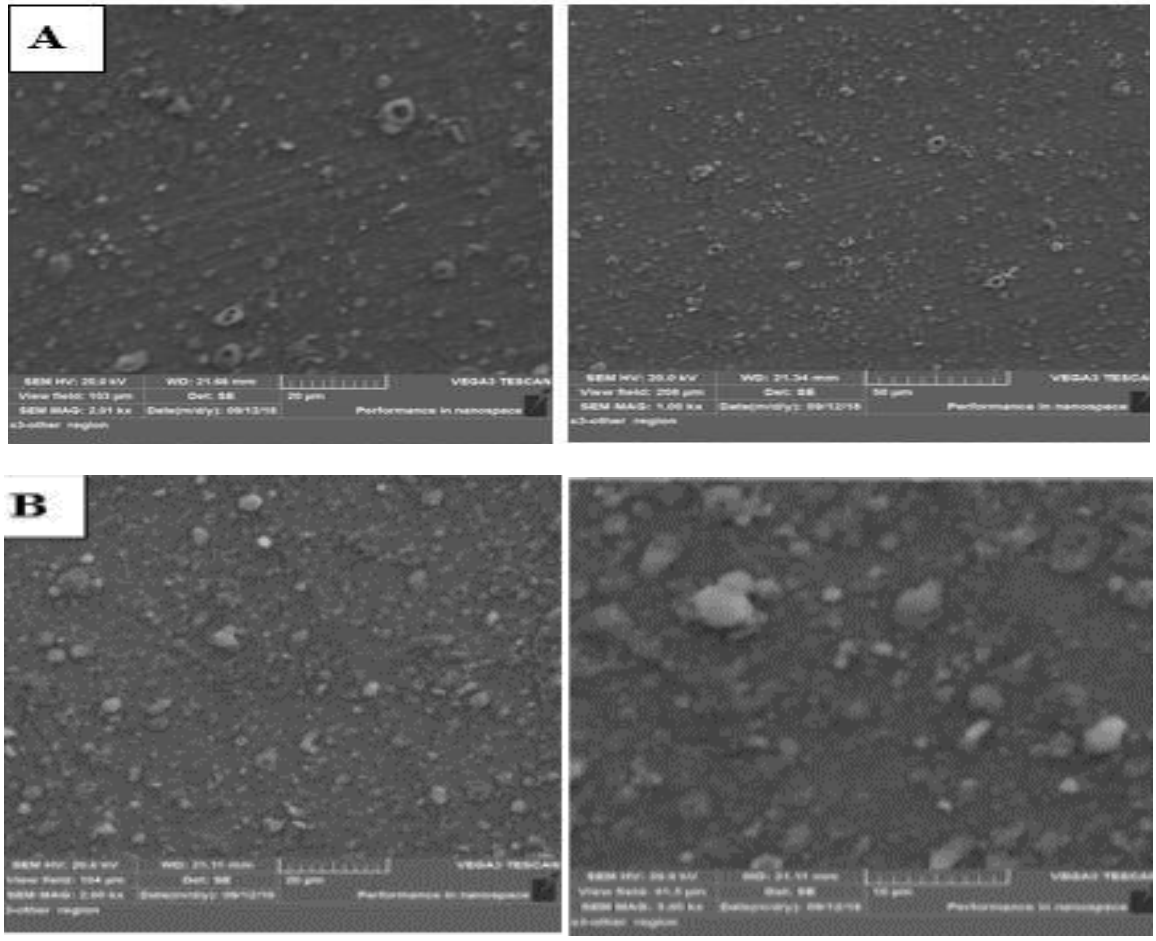

Int. Journal of Integrated Engineering Vol. 16 No. 5 (2024) p. 172-186

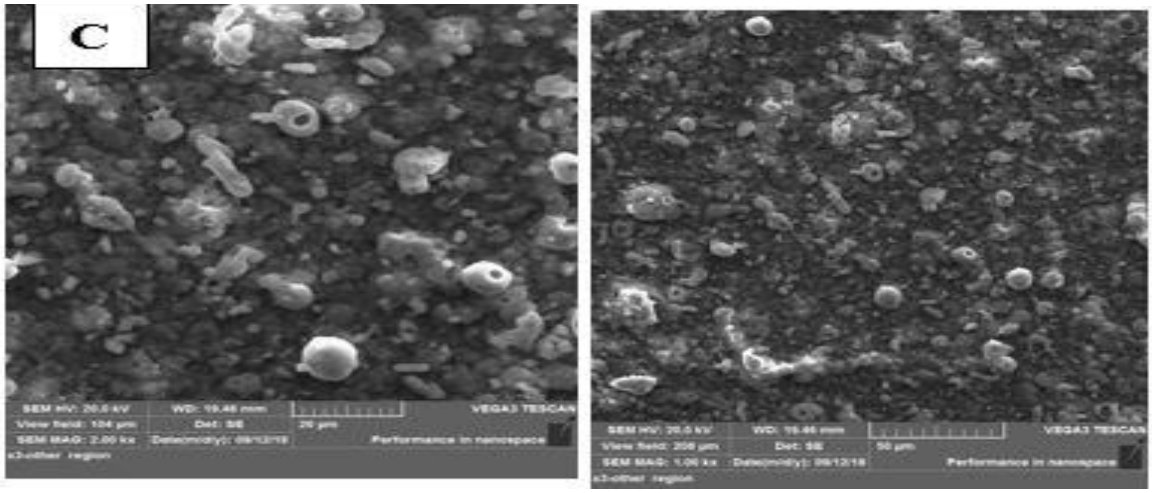

Fig. 9 *SEM micrographs of specimens (a) (Ti-HA-4000); (b) (Ti-HA-6000); and (c) (Ti-HA-8000)*

Energy Dispersive Spectroscopy (EDS) measurement of the as-deposited and treated coatings preserve virtually the same Ca-P proportion (1.62), nearly that of the target material because the coatings are similar to the target material. (1.67). Fig. 9 displays the EDS spectrum of the treated coating obtained from the SEM specimen. Due to the tiny thickness of the coating, it also contains information related to the Titanium substrate [43].

4.6 Histological Results and Discussion

The histological results of the current investigation, from the Hematoxylin and Eosin stain(H&E) under a light Microscope, showed new bone trabeculae formation in all studied groups (control and experimental) (Figs (10-13). The histological section of the control group showed new bone trabeculae lined by osteoblasts and filled by osteocytes. Woven bone and numerous blood vessels are also seen (Fig. 10).

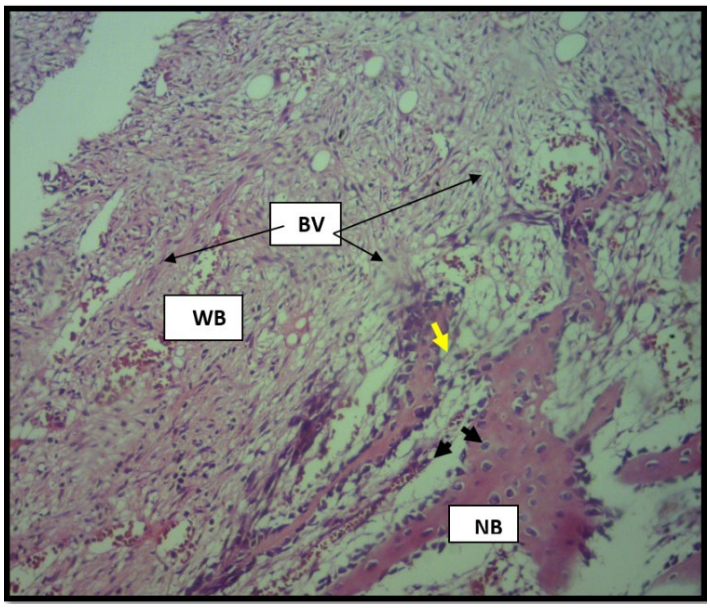

Fig. 10 *Histological view of the control group showed new bone trabeculae (NB) lined by osteoblasts (yellow arrow) and filled by osteocytes (black arrows), woven bone and numerous blood vessels (BV). H&E X10*

The histological picture of the experimental 4000 group revealed a small bone speculum, woven bone with osteoblasts, osteocytes, and many blood vessels in collagenous connective tissue (Fig 11).

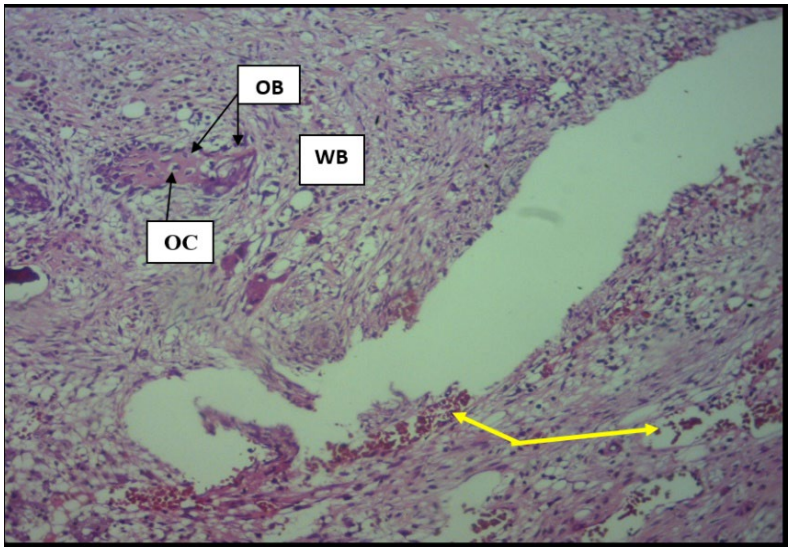

Fig. 11 *Histological view of the experimental 4000 group showed specula of new bone lined by osteoblasts (OB) and filled by osteocytes (OC) and numerous blood vessels (black arrows). H&E X10*

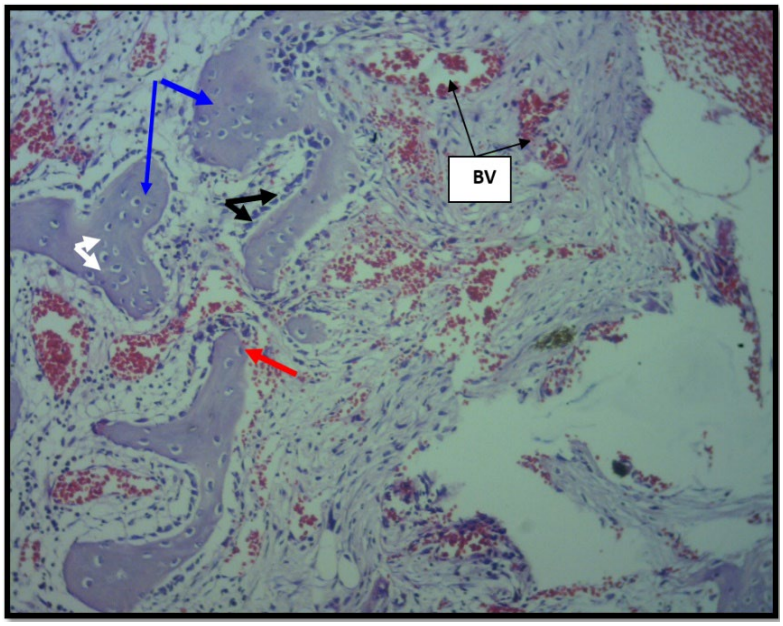

Fig. 12 *Histological view of the experimental 6000 group showed numerous new bone trabeculae (blue arrows) lined by osteoblasts (black arrows), osteoclasts (red arrow) and filled by osteocytes (white arrows), and numerous blood vessels (BV). H&E X10*

The histological view of experimental 6000 groups is a large-sized bone trabecula lined by a single layer of active osteoblasts filled by large-sized osteocytes. Osteoclasts are also seen in the histological section, which may indicate bone re-modelling (Fig 12). On the other hand, the experimental 8000 group showed the best histological result. The section revealed dense, large-sized bone trabeculae separated from basal or old bone by reversal line. Active osteoblasts and multinucleated osteoclasts were seen on the periphery of these bone trabeculae, indicating continuous bone re-modelling. Small-sized osteocytes in their lacunae filled bone trabeculae, and numerous blood vessels could be seen (Fig 13).

Int. Journal of Integrated Engineering Vol. 16 No. 5 (2024) p. 172-186

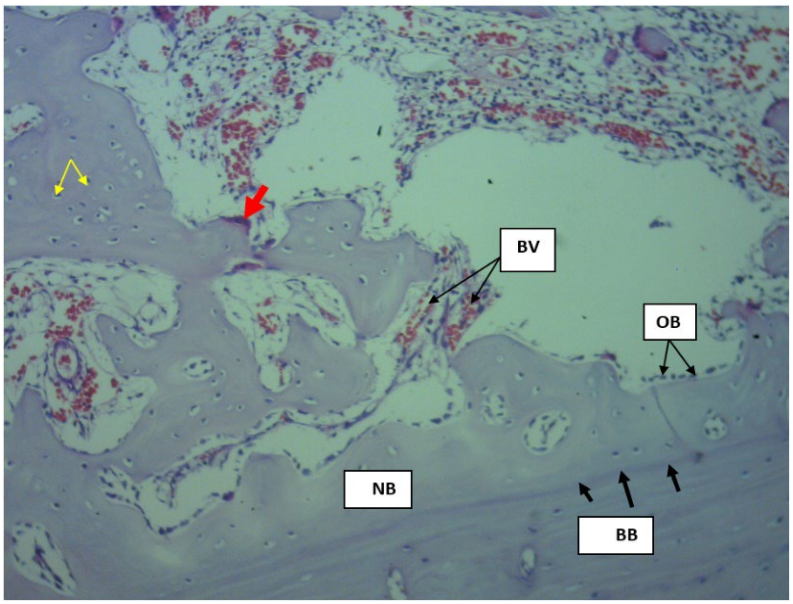

Fig. 13 *Histological view of experimental 8000 group showed dens new bone trabeculae (NB) separated from basal bone (BB) by reversal line (black arrows), osteoblasts (OB), osteoclasts (red arrow) and osteocytes (yellow arrows), and numerous blood vessels (BV). H&E X10*

5. Conclusion

According to the achieved findings, the following conclusions are made:

- Success of the preparation of Hydroxyapatite ($Ca_{10}(PO_4)_6(OH)_2$) by PLD on titanium with thickness (2.2-4.15) µm.
- An increasing number of pulses is more beneficial in film growth and distribution.
- The HA film thickness increased as the number of pulses increased, going from 2.2 µm for the specimen (Ti-HA-4000) to 4.15 µm for the specimen (Ti-HA-8000).
- Surface roughness was found to increase with an increasing number of laser pulses.
- The film's hardness increased from (178 HV to 277 HV) for coated specimens.
- The studies on the coated samples demonstrated an intriguing and significant improvement in biocompatibility compared to the uncoated titanium specimen.
- For the in vivo investigation, the femur bones of four rabbits were implanted with one of four different types of titanium screws (Ti, Ti-HA-4000, Ti-HA-6000, or Ti-HA-8000). The findings demonstrated that fresh bone development surrounding the implant began to occur in both groups at the three-week mark; mature bone formation and full osseointegration occurred around the Ti-HA-8000 implantation at the six-week mark as shown by the existence of Haversian lamellae.

Acknowledgement

This work was supported by Al-Mustaqbal University (grant number MUC-E-0122).

Author contribution statement

The authors confirm contribution to the paper as follows: study conception and design: N. Radhi, H. Jamal Al-Deen; Experimental work and sample preparation: N. Radhi and R. Hadi; present results and analysis of results: Z. Al-Khafaji, N. Radhi, H. Jamal Al-Deen; draft manuscript preparation: Z. Al-Khafaji. All authors reviewed the results and approved the final version of the manuscript.

References

[1] RADHI N.S., AL-KHAFAJI Z., MAREAI B.M., RADHI S., ALSAEGH A.M. (2023) REDUCING OIL PIPES CORROSION BY (ZN-NI) ALLOY COATING ON LOW CARBON STEEL SUBSTRATE BY SUSTAINABLE PROCESS, *Journal of Engineering Science and Technology, 1*8(16), 24–38.

[2] Sattar S., Alaiwi Y., Radhi N.S., Al-Khafaji Z., Al-Hashimi O., Alzahrani H., et al. (2023) Corrosion reduction in steam turbine blades using nano-composite coating, *Journal of King Saud University-Science,* 35(1),102861. https://doi.org/10.1016/j.jksus.2023.102861.

[3] Al-Zubaidy B., Radhi N.S., Al-Khafaji Z.S (2019) Study the effect of thermal impact on the modelling of

(titanium-titania) functionally graded materials by using finite element analysis, *International Journal of Mechanical Engineering and Technology, 10(1), 776–784*. Available online at http://www.iaeme.com/ijmet/issues.asp?JType=IJMET&VType=10&IType=1

[4] Fenech M., Sharma N. (2020) Pulsed laser deposition-based thin film microbatteries, *Chemistry–An Asian Journal,* 15 (12), 1829-1847. https://doi.org/10.1002/asia.202000384

[5] Teghil R., Curcio M., De Bonis A. (2021) Substituted hydroxyapatite, glass, and glass-ceramic thin films deposited by nanosecond pulsed laser deposition (PLD) for biomedical applications: A systematic review, *Coatings*, 11(7), 811. https://doi.org/10.3390/coatings11070811

[6] Badiceanu M., Anghel S., Mihailescu N., Visan A.I., Mihailescu C.N., Mihailescu I.N. (2022) Coatings Functionalization via Laser versus Other Deposition Techniques for Medical Applications: A Comparative Review, *Coatings,* 12(1), 71. https://doi.org/10.3390/coatings12010071

[7] Duta L., Popescu A.C. (2019) Current status on pulsed laser deposition of coatings from animal-origin calcium phosphate sources, *Coatings*, 9 (5), 335. https://doi.org/10.3390/coatings9050335

[8] Yeo I.S.L. (2019) Modifications of dental implant surfaces at the micro-and nano-level for enhanced osseointegration, *Materials*, 13 (1), 89. doi: 10.3390/ma13010089

[9] Hung, K. Y., Lo, S. C., Shih, C. S., Yang, Y. C., Feng, H. P., & Lin, Y. C. (2013) Titanium surface modified by hydroxyapatite coating for dental implants, *Surface and Coatings Technology*, 231(1), 337-345. https://doi.org/10.1016/j.surfcoat.2012.03.037.

[10] Family R., Solati-Hashjin M., Nik S.N., Nemati A. (2012) Surface modification for titanium implants by hydroxyapatite nanocomposite, *Caspian Journal of Internal Medicine*, 3 (3), 460–465.

[11] Radhi, N.S., Kareem, N.E., Al-Khafaji, Z.S., Sahi, N.M. and Falah, M.W., (2022) Investigation mechanical and biological properties of hybrid PMMA composite materials as prosthesis complete denture, *Egyptian Journal of Chemistry*, 65(10), 681-688. DOI: 10.21608/EJCHEM.2022.110545.5034

[12] Dawood N.M., Radhi N.S., Al-khafaji Z.S. (2020) Investigation Corrosion and Wear Behavior of Nickel-Nano Silicon Carbide on Stainless Steel 316L, *Materials Science Forum*, 1002 (1), 33–43. https://doi.org/10.4028/www.scientific.net/MSF.1002.33.

[13] Abed Janabi Z.M., Jaber-Alsalami H.S., Al-Khafaji Z.S., Hussien S.A. (2022) Increasing of the corrosion resistance by preparing the trivalent nickel complex, *Egyptian Journal of Chemistry, 65(6), 193-198*. https://doi.org/10.21608/EJCHEM.2021.100733.4683.

[14] Radhi N.S., Al-Khafaji Z. (2018) Investigation biomedical corrosion of implant alloys in physiological environment, *International Journal of Mechanical and Production Engineering Research and Development,* 8 (4), 247-256. https://doi.org/10.24247/ijmperdaug201827.

[15] Navarro, M., Michiardi, A., Castano, O. and Planell, J.A., (2008) Biomaterials in orthopaedics, *Journal of the royal society interface*, 5(27), 1137-1158. https://doi.org/10.1098/rsif.2008.0151

[16] Hadi R.S., Al-deen H.H.J., Radhi N.S. (2018) Investigation the Coating of Hydroxyapatite on Titanium Substrate by Pulse Laser Deposition, *Journal of University of Babylon for Engineering Sciences*, 26 (10), 299–311.

[17] Balla V.K., Das M., Bose S., Ram G.D.J., Manna I. (2013) Laser surface modification of 316 L stainless steel with bioactive hydroxyapatite, *Materials Science and Engineering: C,* 33(8), 4594-4598. https://doi.org/10.1016/j.msec.2013.07.015

[18] Sallal H.A., Radhi M.S., Mahboba M.H., Al-Khafaji Z. (2022) Impact of embedded sol-gel synthesized triple composites on polymer's mechanical properties, *Egyptian Journal of Chemistry*, 66(6), 197-203. https://doi.org/10.21608/ejchem..154630.6684.

[19] Kwok C.T., Wong P.K., Cheng F.T., Man H.C. (2009) Characterization and corrosion behavior of hydroxyapatite coatings on Ti6Al4V fabricated by electrophoretic deposition, *Applied Surface Science*, 255 (13-14), 6736-6744. https://doi.org/10.1016/j.apsusc.2009.02.086

[20] Jabor M., Radh N.S., Al-kinani M.A., Al-khafaji Z.S. (2021) Optimization of Electro less of Nickel base coating for Cermet Cutting Tools Substrate, *Journal of Mechanical Engineering Research and Developments*, 44 (3), 30–40.

[21] Surmenev R.A., Surmeneva M.A. (2019) A critical review of decades of research on calcium phosphate–based coatings: How far are we from their widespread clinical application?, *Current Opinion in Biomedical Engineering*, 10(1), 35–44. https://doi.org/10.1016/j.cobme.2019.02.003

[22] Fahad N.D., Radhi N.S., Al-Khafaji Z.S., Diwan A.A. (2023) Surface modification of hybrid composite multilayers spin cold spraying for biomedical duplex stainless steel, *Heliyon,* 9(3), e14103. https://doi.org/10.1016/j.heliyon.2023.e14103.

[23] Heimann R.B. (2016) Plasma-sprayed hydroxylapatite-based coatings: chemical, mechanical, microstructural, and biomedical properties, *Journal of Thermal Spray Technology*, 25(1), 827–850. https://doi.org/10.1007/s11666-016-0421-9

[24] Jafari, S., Mahyad, B., Hashemzadeh, H., Janfaza, S., Gholikhani, T., & Tayebi, L. (2020) Biomedical Applications of TiO_2 Nanostructures: Recent Advances, *International Journal of Nanomedicine*, *15 (1)*,

3447–3470. https://doi.org/10.2147/IJN.S249441.
[25] Visentin F., El Habra N., Fabrizio M., Brianese N., Gerbasi R., Nodari L., et al. (2019) TiO2-HA bi-layer coatings for improving the bioactivity and service-life of Ti dental implants, *Surface and Coatings Technology*, 378 (1), 125049. https://doi.org/10.1016/j.surfcoat.2019.125049
[26] Narayanan, R., Seshadri, S.K., Kwon, T.Y. and Kim, K.H., (2008) Calcium phosphate ‐ based coatings on titanium and its alloys. Journal of Biomedical Materials Research Part B: Applied Biomaterials: An Official Journal of The Society for Biomaterials, *The Japanese Society for Biomaterials, and The Australian Society for Biomaterials and the Korean Society for Biomaterials*, 85(1), 279-299. https://doi.org/10.1002/jbm.b.30932
[27] Kwiatkowska, J., Suchanek, K. and Rajchel, B., 2012. Bioactive glass coatings synthesized by pulsed laser deposition technique, *Acta Physica Polonica A*, 121(2), 502-505.
[28] Zheng, K. and Boccaccini, A.R., (2017) Sol-gel processing of bioactive glass nanoparticles: A review, *Advances in Colloid and Interface Science*, 249 (1), 363-373. https://doi.org/10.1016/j.cis.2017.03.008
[29] Rajesh, P., Mohan, N., Yokogawa, Y. and Varma, H., (2013) Pulsed laser deposition of hydroxyapatite on nanostructured titanium towards drug eluting implants, *Materials Science and Engineering: C*, 33(5), 2899-2904. https://doi.org/10.1016/j.msec.2013.03.013
[30] Salih, E.M., Karim, H.J., Al-Sultani, K.F. and Al-Khafaji, Z., (2024) Effect of Ge on oxidation behavior of 60% Cu–40% Zn Muntz metal, *Engineering Review: Međunarodni časopis namijenjen publiciranju originalnih istraživanja s aspekta analize konstrukcija, materijala i novih tehnologija u području strojarstva, brodogradnje, temeljnih tehničkih znanosti, elektrotehnike, računarstva i građevinarstva*, 44(1), 25-37. https://doi.org/10.30765/er.2201
[31] Kadhim, I. A. U., Sallal, H. A., & Al-Khafaji, Z. S. (2023) A review in investigation of marine biopolymer (chitosan) for bioapplications, *ES Materials & Manufacturing,* 21, 828. DOI:10.30919/esmm5f828
[32] Rajesh, P., Muraleedharan, C. V., Komath, M., & Varma, H. (2011) Pulsed laser deposition of hydroxyapatite on titanium substrate with titania interlayer, *Journal of Materials Science: Materials in Medicine*, *22 (1)*, 497-505. https://doi.org/10.1007/s10856-011-4230-x
[33] Wu, C., Tang, Y., Mao, B., Zhao, K., Cao, S., & Wu, Z. (2021) Rapid apatite induction of polarized hydrophilic HA/PVDF bio-piezoelectric coating on titanium surface, *Surface and Coatings Technology*, *405 (1)*, 126510. https://doi.org/10.1016/j.surfcoat.2020.126510
[34] Lyu, L., Yang, S., Jing, Y., Zhang, C., & Wang, J. (2020) Examining trabecular morphology and chemical composition of peri-scaffold osseointegrated bone, *Journal of Orthopaedic Surgery and Research*, 15 (1), 1-9. https://doi.org/10.1186/s13018-020-01931-z
[35] Nazir, M., Pei Ting, O., See Yee, T., Pushparajan, S., Swaminathan, D., & Kutty, M. G. (2015) Biomimetic coating of modified titanium surfaces with hydroxyapatite using simulated body fluid, *Advances in Materials Science and Engineering*, 2015 (1), 8. https://doi.org/10.1155/2015/407379
[36] Bansal, P., Singh, G., & Sidhu, H. S. (2021) Improvement of surface properties and corrosion resistance of Ti13Nb13Zr titanium alloy by plasma-sprayed HA/ZnO coatings for biomedical applications, *Materials Chemistry and Physics*, 257, 123738. https://doi.org/10.1016/j.matchemphys.2020.123738
[37] Baltatu, M. S., Vizureanu, P., Sandu, A. V., Munteanu, C., & Istrate, B. (2020), Microstructural analysis and tribological behavior of Ti-based alloys with a ceramic layer using the thermal spray method, *Coatings*, 10(12), 1216. https://doi.org/10.3390/coatings10121216
[38] Cavalu, S., Simon, V., Ratiu, C., Oswald, I., Gabor, R., Ponta, O., Akin, I. and Göller, G., (2012) Correlation between structural properties and in vivo biocompatibility of alumina/zirconia bioceramics. *Key Engineering Materials*, *493*, 1-6. https://doi.org/10.4028/www.scientific.net/KEM.493-494.1
[39] An, Y. H., & Martin, K. L. (Eds.). (2003) Handbook of histology methods for bone and cartilage (pp. 361-374). Totowa, NJ: Humana Press.
[40] Van Pelt, L. (1977) Ketamine and xylazine for surgical anesthesia in rats, *Journal of the American Veterinary Medical Association*, *171*(9), 842-844.
[41] Radhi, N. S. (2018) Preparation and modeling (titanium-hydroxyapatite) functionally graded materials for bio-medical application, *International Journal of Civil Engineering and Technology*, *9*(6), 28-39.
[42] Rajesh, P., Muraleedharan, C. V., Manoj, K., & Varma, H. K. (2007) Coating of hydroxyapatite on titanium at 200ºC by pulsed laser deposition and hydrothermal annealing, *Bulletin of Materials Science*.
[43] Komath, M., Rajesh, P., Muraleedharan, C. V., Varma, H. K., Reshmi, R., & Jayaraj, M. K. (2011) Formation of hydroxyapatite coating on titanium at 200 C through pulsed laser deposition followed by hydrothermal treatment, *Bulletin of Materials Science*, *34 (1)*, 389-399. https://doi.org/10.1007/s12034-011-0069-5